Effect of copper doping on the optical and dielectric parameters of glycine zinc sulfate (GZS) single crystals

Abduh Mohammed Abdulwahab[a,*], Ahmad Ali Qaid[b], Tawfik Mahmood Mohammed Ali [c] and Annas Saeed Al-Sharabi [a]

a- Physics Department, Faculty of Applied Science, Thamar University, Dhamar 87246, Yemen
b- Chemistry Department, Faculty of Applied Science, Thamar University, Dhamar 87246, Yemen
c- Physics Department, Al-Dalaa Faculty of Education, University of Aden, Aden, Yemen
E-mail address: abduhabdulwahab@yahoo.com
DOI: https://doi.org/10.47372/uajnas.2021.n2.a09

Abstract

Glycine zinc sulfate (GZS) single crystals pure and doped with copper were grown by the slow evaporation of aqueous solutions at constant temperature (307 K). Cu/Zn molar ratios were 1%, 2% and 3% in the growth solutions. The optical reflectance was measured for pure and doped crystals (GZS:Cu) and it was used to calculate several optical and dielectric parameters. The direct optical band gap energy was found to be 5.44 eV for pure GZS crystal and it decreased as Cu/Zn molar ratio increased. The band tailing was studied for GZS:Cu crystals by using Urbach relation. The normal dispersion was investigated for GZS:Cu crystals by using both Wemplee–Di-Domenico and Cauchy-Sellmaier models. The real and imaginary parts of the complex dielectric constant of GZS:Cu crystals were calculated. Urbach parameters, normal dispersion parameters and dielectric parameters of GZS:Cu crystals were calculated in the present work for the first time. It was found that doping GZS crystal, with copper, affects the values of its optical and dielectric parameters and improves its electrical conduction.

Keywords: GZS single crystal; Copper–doped; Band gap; Normal dispersion; Dielectric constant.

1. Introduction

Glycine zinc sulfate (GZS) crystal is semi-organic nonlinear optical (NLO) material and many studies have been achieved on it because of its practical applications in harmonic generation, switching and other optical signal processing devices [6, 14, 21, 23]. GZS crystal belongs to orthorhombic system and the cell parameters are a = 8.440(2) Å, b = 8.278(2) Å, c = 12.521(3) Å and V = 874.8(4) Å^3 [9, 23]. The electron paramagnetic resonance (EPR) of copper ions has been studied as paramagnetic impurity in GZS single crystal at ambient temperature [20]. The detailed (EPR) analysis showed the only one site of Cu (II) and entered the lattice substitutionally in place of Zn (II) [20].

The optical band gap energy (E_g) and some optical constants have been calculated for GZS crystal in some articles. Indirect E_g was reported as 3.8 eV [4], while direct E_g was reported as 4.25 eV [22], 4.55 eV [7] and 5.4 eV [17]. Some optical constants have been calculated, such as refractive index (n) ,which was reported as 1.587 at λ = 1000 nm and extinction coefficient ($K_{ex.}$) which was found to be 4.15 × 10^{-6} at λ = 1000 nm [17]. GZS crystal has been doped with cobalt [4] and it was found that indirect optical band gap energy (E_g) decreases with increasing cobalt content.

Recently, linear and nonlinear optical properties of glycine zinc sulfate (GZS) crystal have attracted the attention of many researchers [10, 25, 26]. Vijayalakshmi and Dhanasekaran [25] grew single crystals of different molar ratios of $ZnSO_4$-added glycine by using the slow evaporation method. They reported that the nonlinear optical property improves for 0.6 M of $ZnSO_4$-added glycine and the direct E_g of 1 M of $ZnSO_4$-added glycine (GZS) crystal equals to 5.933 eV. The same researchers studied the linear and nonlinear optical properties of glycine and

zinc sulphate mixed crystal in the molar ratio 1:0.7 respectively. They found that the second harmonic generation efficiency of this crystal increases and the direct E_g value is 5.99 eV [26]. In growing GZS single crystal by using Sanakaranarayan - Ramasamy (SR) technique and studying by physical properties for optoelectronic applications, it was found that the grown crystal has 80% transparency in the wavelength range of 300–950 nm. They confirmed the application of GZS in NLO devices and they reported that the direct E_g = 4.6 eV [10].

To the best of our knowledge, the works on the linear optical properties of GZS crystal are scarce and some important optical and dielectric parameters have not been calculated yet for this crystal. On the other hand, copper had been used as impurity in GZS single crystal [20] but the effect of this impurity on the linear optical properties of the crystal has not been studied yet. Moreover, the absorption coefficient (α) and the optical energy gap (E_g) of GZS crystal have not been calculated yet by using the reflection spectra. Therefore, in the present work, we will use the reflectance measurements to calculate several optical and dielectric parameters of GZS crystal and to study the effect of copper as dopant on these parameters.

2. Experimental details

Synthesis

Pure glycine zinc sulfate (GZS) compound was synthesized as an aqueous solution by dissolving glycine (NH_2CH_2COOH) and zinc sulfate heptahydrate ($ZnSO_4{\cdot}7H_2O$) in the molar ratio 1:1 in double distilled water according to the following reaction [23]:

$$NH_2CH_2COOH + ZnSO_4{\cdot}7H_2O \rightarrow Zn[NH_2CH_2COOH]SO_4{\cdot}3H_2O + 4H_2O \quad (1)$$

Copper–doped GZS compounds were synthesized as aqueous solutions by adding copper sulfate pentahydrate ($CuSO_4{\cdot}5H_2O$), as a source of Cu dopant, to the solution of pure GZS with different molar ratios separatelly. Cu concentrations or Cu to Zn molar ratios (Cu/Zn) in the solution of growth were 1%, 2% and 3%. In general, we will refer to our samples in this paper as GZS:Cu where the pure (undoped) sample (GZS) has Cu/Zn molar ratio of 0% and the copper–doped samples have three different Cu/Zn molar ratios 1%, 2% and 3% in the solution of growth .

Crystal Growth

All aqueous solutions were evaporated slowly at room temperature for several days to obtain seeds and then clear seeds were chosen to grow single crystals. The aqueous solutions have been supersaturated at constant temperature (307 K) and these supersaturated solutions have been used to grow pure and copper–doped GZS single crystals by the slow evaporation technique. Crystal growth process was achieved by using an indigenous crystal growth apparatus (crystallizer). To grow all crystals simultaneously at the same conditions, the crystallizer was multi-jar. Optimum growth parameters including solution purity, seed orientation and purity, seed rotational speed, temperature of crystallization, and period of growing crystal were chosen for the best result.

Optical Measurements

For optical measurements, the samples were prepared from the obtained single crystals as rectangular plates 1 mm in thickness. The samples were polished by using a wet soft cloth. The obtained samples were clear, transparent, and free from noticeable defects. The optical reflectance was recorded for all samples with unpolarized monochromatic light using UV-Visible spectrophotometer (Varian, Cary 50). The measurements were performed at room temperature in the wavelengths range of 200–800 nm and the air was the surrounding medium.

3. Results and discussion

Reflectance spectra

In Fig. 1, the optical reflectance (R) is plotted as a function of wavelength (λ) for GZS:Cu crystals. One can see that, at the whole measured range of wavelengths, all crystals have small

reflectance ($R < 0.06$) and it decreased as Cu amount increased. This behavior may be caused by increasing free charge carriers and, therefore, increasing the distortion which leads to decreasing the reflectance of the crystal.

Absorption coefficient

For the samples having large thickness, compared with the wavelength, the absorption coefficient (α) can be obtained from the measured reflectance (*R)* by using the following formula [13]:

$$\alpha = Ln\left(\frac{(R_{max.}-R_{min.})}{(R-R_{min.})}\right)/2t \quad (2)$$

where $R_{max.}$ and $R_{min.}$ are the maximum and minimum reflectance values in reflection spectra, R is the recorded reflectance value for any intermediate wavelength and t is the sample thickness. The photon energy (E) can be calculated from the wavelength (λ) by using the known formula:

$$E = hc/\lambda \quad (3)$$

where h is Planck constant and c is the velocity of light in vacuum.

In the present work, each sample used for reflectance measurements has a thickness of 1 mm which is large when comparing it with the used wavelengths range (200–800 nm). Therefore, our samples obey the condition to calculate the absorption coefficient (α) by using Eq. (2). The relation between absorption coefficient (α) and photon energy (E), for GZS:Cu crystals, is shown in Fig. 2. It is clear that, for all GZS:Cu crystals, α increased with increasing E and it increased more rapidly when E became more than a special value called the optical band gap energy (E_g). In addition, one can see that the absorption coefficient

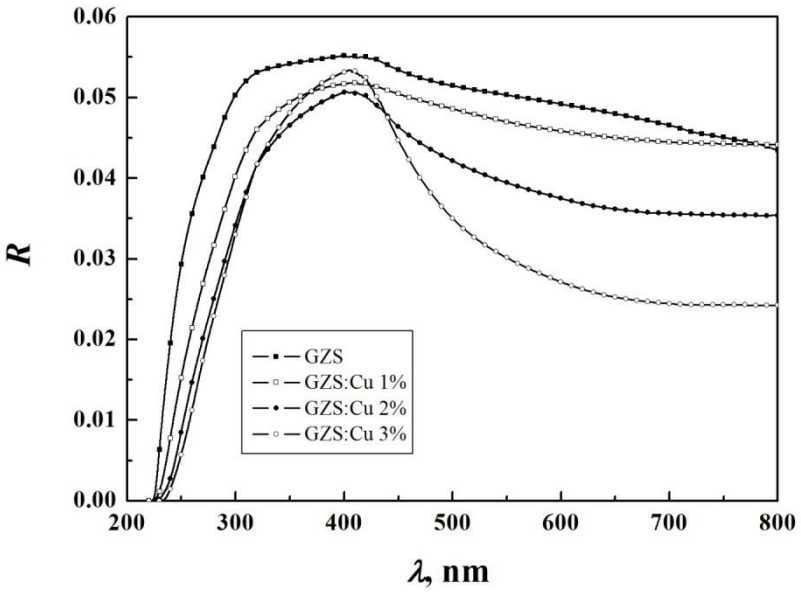

Fig. 1. The reflectance spectra versus wavelength (λ) for GZS:Cu crystals.

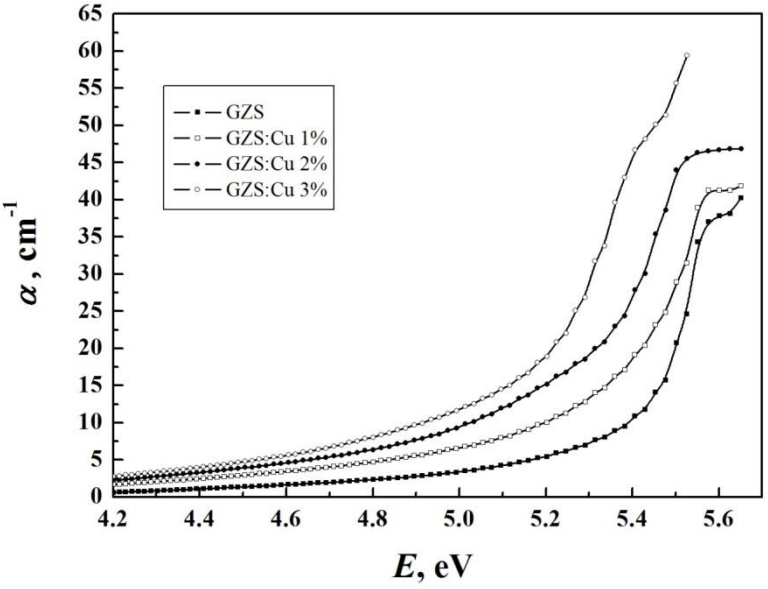

Fig. 2. The absorption coefficient (α) versus photon energy (E) for GZS:Cu crystals.

(α) increased with increasing Cu/Zn molar ratio. This behavior can be related to increasing defects in the doped crystals.

Optical band gap energy

The relation between absorption coefficient (α) and photon energy (E) has the following formula [15]:

$$\alpha E = B\left(E - E_g\right)^n \quad (4)$$

where B is a constant depends on electron and hole effective masses of the material and n refers to the type of transition (n = 1/2 for direct allowed transition, n = 3/2 for direct forbidden transition, n = 2 for indirect allowed transition and n = 3 for indirect forbidden transition). For the present work, the best linear fitting was obtained with n = 1/2 and so GZS:Cu crystals have the allowed direct transition. The plots of $(\alpha E)^2$ versus E for GZS:Cu samples are shown in Fig. 3. The straight lines of these plots were extended to E axis to obtain the values of direct optical band gap energy (E_g) and the obtained values are listed in Table 1.

The value of E_g obtained in this work for pure GZS crystal (5.44 eV) agrees well to that (5.4 eV) reported by Nithya et al. [17]. In some other publications, E_g of pure GZS crystal has slightly different values. The differences in E_g value in those works can be explained by the differences in crystal growth conditions from one work to another [7, 10, 22, 25, 26]. These conditions are equivalent in the present work and in the work of Nithya et al. [17]. Therefore, E_g has approximately the same value in the two works.

It is clear that the optical band gap energy decreased with increasing Cu/Zn molar ratio. This behavior may be related to increasing defects in the doped crystals which leads to increasing free charge carriers. The obtained values of optical band gap energy (E_g) for GZS:Cu crystals (5.44–5.17 eV) indicate that GZS is insulator. Copper ions incorporated in the lattice of GZS crystal as impurities and the carriers of free charge increased and, therefore, E_g decreased. This means that doping GZS crystal with copper, leads to decreasing its insulating property i.e. improving the electrical conduction of the crystal.

Urbach rule

Under optical band gap energy, the absorption coefficient (α) can be obtained by using the empirical Urbach relation [24]:

$$\alpha = \alpha^* exp\left(\frac{E-E^*}{E_U}\right) \quad (5)$$

where α^* and E^* are characteristic parameters depend on the material, E is the incident photon energy and E_U is the band tail energy or Urbach energy which characterizes the width of the located states. The region of photon energies ,where α obeys Eq. (5), is called the Urbach tail range. Urbach energy (E_U) depends on temperature (T) by the following relation [12]:

$$E_U = \frac{K_B T}{\sigma} \quad (6)$$

where K_B is the Boltzmann constant and σ is a steepness parameter which characterizes the width of the straight line near the absorption edge. Eq. (5) can be changed to the form:

$$Ln(\alpha) = Ln(\alpha^*) + \left(\frac{E-E^*}{E_U}\right) \quad (7)$$

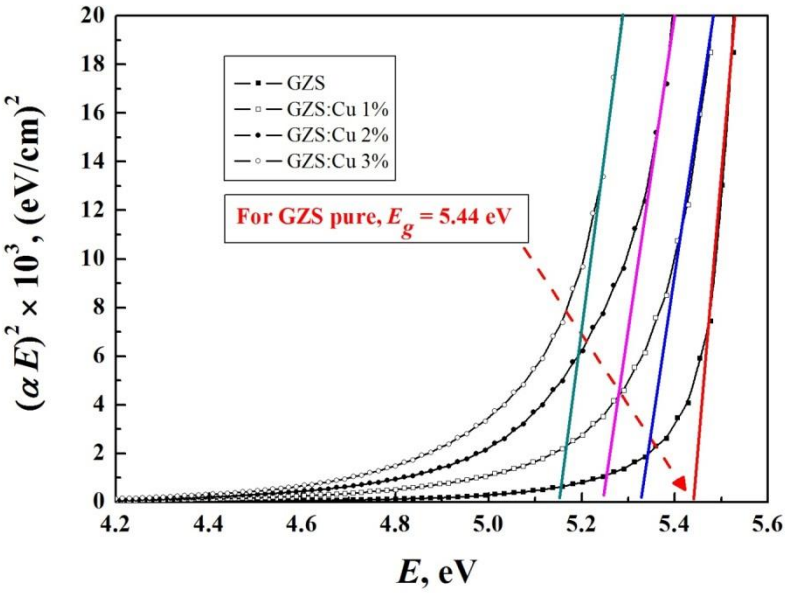

Fig. 3. $(\alpha E)^2$ versus photon energy (E) for GZS:Cu crystals.

Therefore, plotting $Ln(\alpha)$ against E at the Urbach tail range gives a straight line which has a slope of $1/E_U$ and intersection of $Ln\ (\alpha^*) - E^*/E_U$. If the relation between α and E is of the Urbach type, the obtained straight lines at a wide range of $Ln(\alpha)$~E graph will converge to the same point [E^*, $Ln\ (\alpha^*)$].

In Fig. 4, the dependence of $Ln\ (\alpha)$ on E is displayed for GZS:Cu crystals. The range of E in part (a) is less than E_g (the Urbach tail range) ,while in part (b) there is a wide range of E more than E_g.

The obtained relations were fitted to the best straight lines according to Eq. (7) by using Origin program. Part (a) shows clearly the straight lines of $Ln(\alpha)$~E relations. From the slopes of these straight lines, the Urbach energy (E_U) was calculated for each sample and then, by using Eq. (6), the steepness parameter (σ) was calculated from E_U at constant temperature (T = 298 K). Part (b) shows that the obtained straight lines for GZS:Cu crystals converged to the same point [E^*, $Ln\ (\alpha^*)$]. The obtained values of E_U, σ, E^*, $Ln\ (\alpha^*)$ and α^* are listed in Table 1.

Table 1: Optical band gap energy and Urbach parameters for GZS:Cu crystals.

	E_g, eV	E_U, eV	σ	E^*, eV	Ln (α^*)	α^*, cm^{-1}
GZS	5.44	0.39	0.0667	6.5	4.9	134.3
GZS:Cu 1%	5.33	0.53	0.0485			
GZS:Cu 2%	5.25	0.55	0.0470			
GZS:Cu 3%	5.17	0.56	0.0458			

The values of Urbach energy (E_U) for copper–doped GZS crystals are more than that for the pure one, while the values of steepness parameter (σ) for copper–doped GZS crystals are less than that for the pure one. This behavior, for both E_U and σ, is conceivable because of the increase in disorder and defects in the doped GZS crystals.

It is clear from Table 1 and Fig. 4 (b) that each of E^* and α^* parameter has only one value for all samples. this is because the two parameters (E^* and α^*) depend only on the material, but not on dopant molar ratio. Moreover, if we doped GZS crystal with any other material or using any influent, like heating, and we obtained Urbach tail, the values of both E^* and α^* will stay the same. This means that, E^* and α^* parameters are independent of the dopant type or on heating. This behavior of E^* and α^* parameters was tested for another crystal (ZTS) in the previous two works [2, 3]. The influent was heated in one work [3] and doped with cobalt in the other work [2], but the values of both E^* and α^* were the same in the two works.

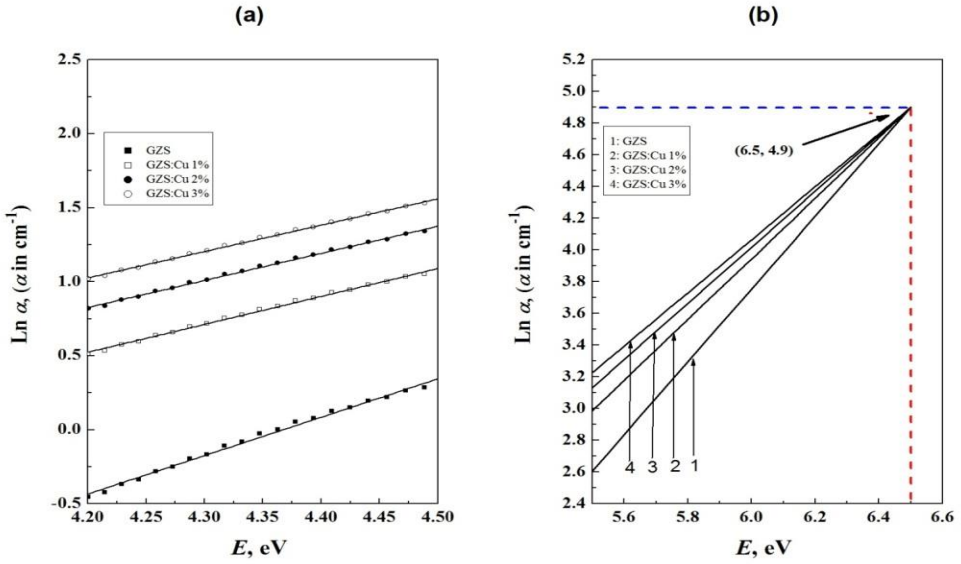

Fig. 4. Ln (α) versus photon energy (E) for GZS:Cu crystals. (a) In narrow range of E less than E_g. (b) In wide range of E more than E_g.

Both E_g and E_U are shown in Fig. 5 as a function of Cu/Zn molar ratio in the growth solution of GZS:Cu crystals. One can see that the optical band gap (E_g) changed reversely with Urbach energy (E_U). This behavior leads to a possible redistribution of states [18].

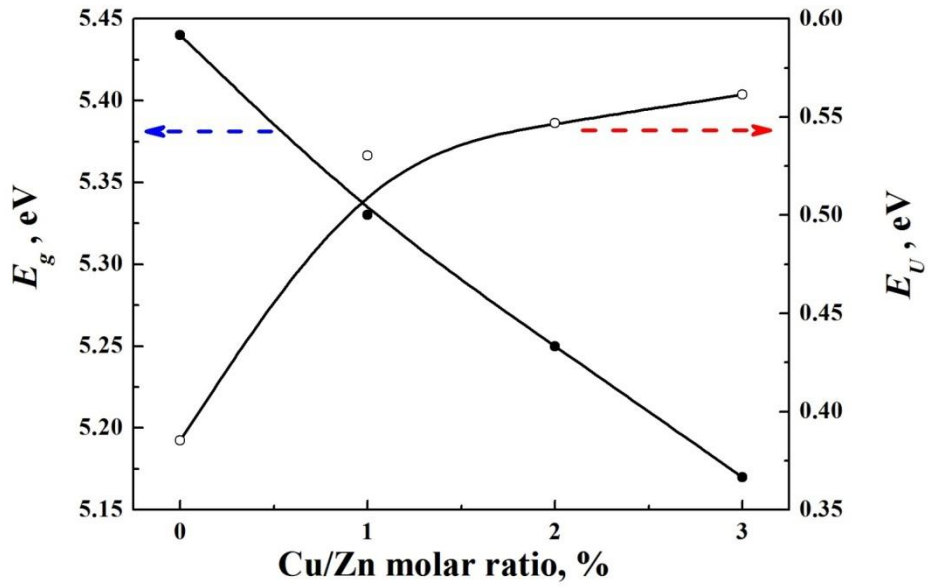

Fig. 5. Variations of the optical energy gap (E_g) and Urbach tail energy (E_U) with Cu/Zn molar ratio in the growth solution of GZS:Cu crystals.

Extinction coefficient and refractive index

The extinction coefficient ($K_{ex.}$) and refractive index (n) can be calculated from α, λ and R by using the following relations [1]:

$$K_{ex.} = \frac{\alpha\lambda}{4\pi} \quad (8)$$

$$R = \frac{(n-1)^2+K_{ex.}^2}{(n+1)^2+K_{ex.}^2} \quad (9)$$

Since $K_{ex.}$ is very small, Eq. (9) can be written as the following simple form:

$$n = \frac{(1+\sqrt{R})}{(1-\sqrt{R})} \quad (10)$$

The obtained values of $K_{ex.}$ and n for GZS:Cu crystals are plotted as functions of photon energy (E) in Fig. 6 and Fig. 7 respectively. It is clear that, for all GZS:Cu crystals and for all measured range of photon energies, the values of the extinction coefficient ($K_{ex.}$) are between 0 and 11×10^{-5} ,while the values of the refractive index (n) are between 1 and 1.62. Furthermore, $K_{ex.} \cong 10^{-5}\, n$ at all measured E range and for all GZS:Cu crystals. The values of both $K_{ex.}$ and n for pure GZS crystal are in very good agreement with those ($K_{ex.}$ = 4.15 × 10^{-6} and n = 1.587 at λ = 1000 nm) reported by Nithya et al. [17].

Fig. 6 shows that the extinction coefficient ($K_{ex.}$) increased with increasing Cu/Zn molar ratio at all measured range of photon energies. This behavior may be explained by the increase of defects in the doped

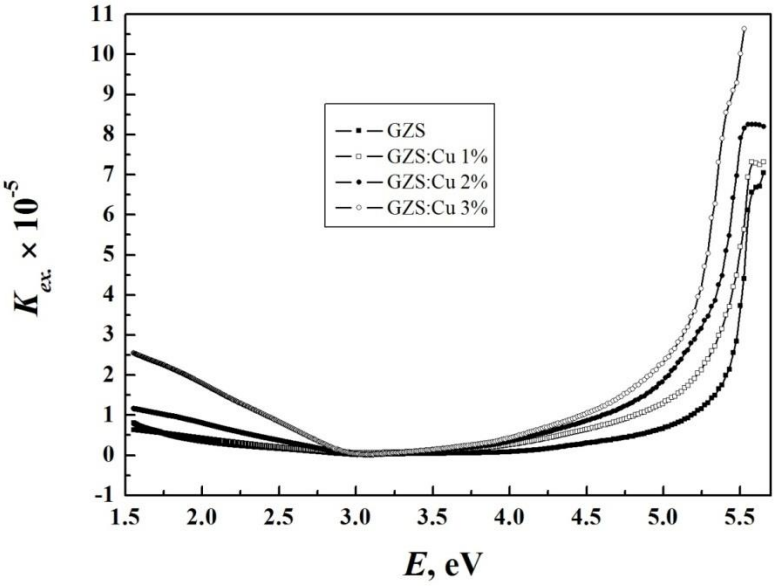

Fig. 6. Extinction coefficient ($K_{ex.}$) versus photon energy (E) for GZS:Cu crystals.

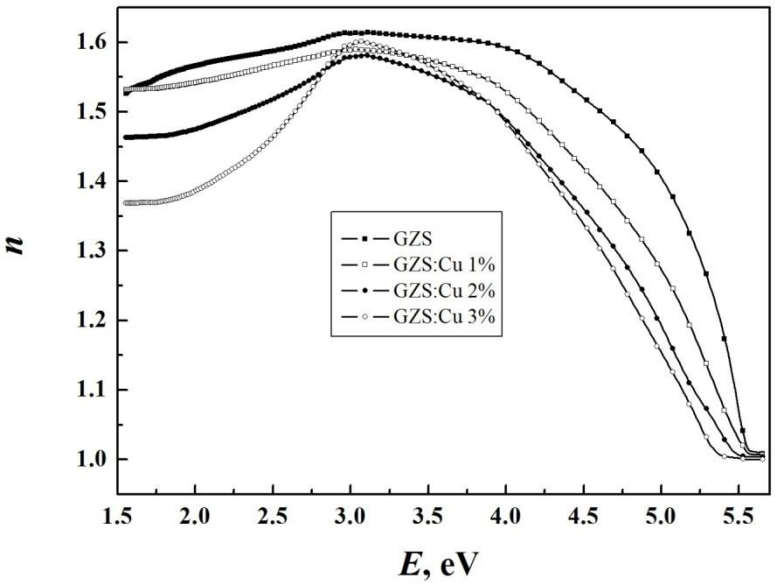

Fig. 7. Refractive index (n) versus photon energy (E) for GZS:Cu crystals.

crystals. In addition, the extinction coefficient ($K_{ex.}$) decreased with increasing photon energy (E) at the lower photon energies for all GZS:Cu crystals. But, it has a rapid increase with increasing photon energy (E) at the higher photon energies. This behavior can be explained by fundamental absorption edge of the material which lies in this range of E.

As seen in Fig. 7, the refractive index (n) decreased with increasing Cu/Zn molar ratio at all measured range of photon energies. This behavior is caused by the increase of distortion in the doped crystals. Furthermore, the refractive index (n) increased with increasing photon energy (E) at the lower photon energies for all GZS:Cu crystals. At the higher photon energies, n decreased

rapidly with increasing photon energy (*E*). This behavior will be discussed and explained with more details in the following section.

Normal dispersion and its parameters

Dispersion is defined as the dependence of refractive index (*n*) on photon energy (*E*). It has an importance in the optical studies because it is a major factor in some optical applications like optical communication and designing devices for spectral dispersion [16].

One can see in Fig. 7 that the refractive index (*n*) of GZS:Cu crystals increased with increasing photon energy (*E*) when *E* is less than 3 eV. This range of *E* is below the fundamental absorption edge of the material (E_g > 5 eV). This behavior of *n* refers to the presence of normal dispersion at this range of photon energies. When *E* is more than 3 eV, *n* decreased with increasing *E*. This behavior of *n* refers to the presence of anomalous dispersion at this range of photon energies, in addition to the effect of fundamental absorption edge of the material [11, 28].

The relation between the refractive index (*n*) and photon energy (*E*) can be described by using the single oscillator model developed by Wemple and DiDomenico. According to this model, *n* has the following relation with *E* [27]:

$$n^2 = 1 + \frac{E_0 E_d}{E_0^2 - E^2} \quad (11)$$

where E_0 is the single oscillator energy and E_d is the dispersion energy. The materials can be known if they are different in their structures and optical constants by differing of E_0 and E_d [5]. We can change Eq. (11) to the following form:

$$(n^2 - 1)^{-1} = \left(\frac{E_0}{E_d}\right) - \left(\frac{1}{E_0 E_d}\right) E^2 \quad (12)$$

Sketching $(n^2\text{-}1)^{-1}$ as a function of E^2 would give a straight line which has a negative slope $1/E_0E_d$ and intersection E_0/E_d. Such relations for GZS:Cu crystals are shown in Fig. 8 (a) at all measured range of photon energies. Fig. 8 (b) shows that the obtained relations were fitted to the best straight lines according to Eq. (12), by using Origin program at E^2 range of 4–6 eV^2 (*E* range of 2–2.45 eV) which occurs at the normal dispersion region. The fitted relations give excellent straight lines for all samples and, therefore GZS:Cu crystals have normal dispersion at this range of photon energies according to Wemple and DiDomenico dispersion relation. The slopes and intersections of the straight lines were used to calculate E_0 and E_d for all samples and the obtained values are listed in Table 2.

Table 2: Normal dispersion parameters for GZS:Cu crystals.

	E_o, eV	E_d, eV	f, $(eV)^2$	M_{-1}	M_{-3}, $(eV)^{-2}$	a_1, $(eV)^{-2}$	n_o
GZS	7.408	10.01	74.15	1.3510	0.0246	0.00943	1.53
GZS:Cu 1%	6.822	8.586	58.57	1.2587	0.0271	0.01093	1.50
GZS:Cu 2%	5.165	5.163	26.67	0.9996	0.0375	0.01897	1.40
GZS:Cu 3%	3.976	2.736	10.88	0.6882	0.0435	0.03286	1.25

One can see that the single oscillator energy (E_0) decreased with increasing Cu/Zn molar ratio. This indicates that the normal dispersion region shifts to a range of lower photon energies for doped samples. Also, increasing Cu/Zn molar ratio leads to decreasing the dispersion energy (E_d) which indicates that the intensity of the inter-band optical transitions decreased for doped samples. The changes of E_0 and E_d values by doping GZS crystal with copper are related to the changes of chemical bonds and their bonding energy caused by presence of Cu ions [16].

The oscillator strength (*f*) can be obtained from the values of E_0 and E_d by using the following relation [8]:

$$f = E_0 \times E_d \quad (13)$$

The values of oscillator strength (*f*) for GZS:Cu crystals are listed in Table 2.

The optical spectrum moments (M_{-1} and M_{-3}) are related to E_0 and E_d by the following two equations [8]:

$$E_0^2 = \frac{M_{-1}}{M_{-3}} \quad (14)$$

$$E_d^2 = \frac{M_{-1}^3}{M_{-3}} \quad (15)$$

These two equations were used, with the values of E_0 and E_d, to calculate M_{-1} and M_{-3} for GZS:Cu samples and the obtained values are listed in Table 2. It is clear that ,when Cu/Zn molar ratio increases, M_{-1} value decreases, while the value of M_{-3} increases.

Dependence n on E at normal dispersion region ($E < E_g$) can be described by the approximated Cauchy-Sellmaier equation expanded in even powers of photon energy (E). The first approximation of this function is of the following form [8]:

$$n = n_0 + a_1 E^2 \quad (16)$$

where n_0 and a_1 are Cauchy coefficients that depend on the material. The parameter a_1 represents the dispersion $dn/d(E)^2$ of the material and n_o is the static refractive index of the material (the refractive index at $E = 0$). Plotting n as a function of E^2 will give a straight line with a slope a_1 and intersection n_0.

The relations between n and E^2 for GZS:Cu crystals are shown in Fig. 9 (a) at all measured range of photon energies. Fig. 9 (b) shows that the obtained relations were fitted to the best straight lines according to Eq. (16), by using Origin program at E^2 range of 4–6 eV^2 (E range of 2–2.45 eV) which occurs at the normal dispersion region. The fitted relations give excellent straight lines for all samples and, therefore the optical data of GZS:Cu crystals obey Cauchy–Sellimaier dispersion equation at this photon energies range (the normal dispersion region). Cauchy coefficients a_1 and n_0 were obtained, respectively from the slopes and intersections of the straight lines for all studied samples and their values are listed in Table 2. The parameter a_1 increased, while n_0 decreased with increasing Cu/Zn molar ratio. This means that when the copper content increased in GZS crystal as dopant, the dispersion (dn/dE) of the crystal increased and the refractive index at $E = 0$ decreased.

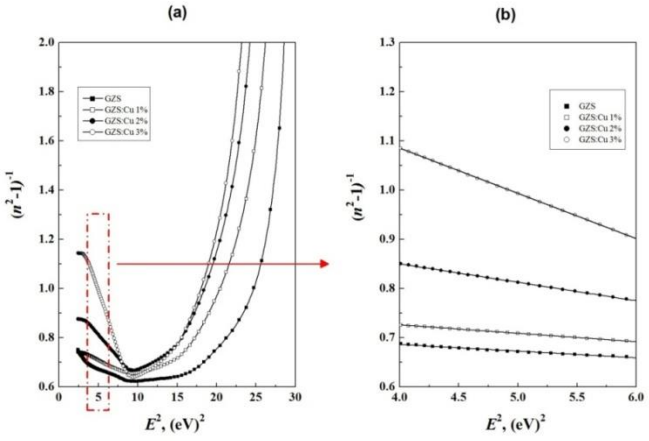

Fig. 8. $(n^2-1)^{-1}$ versus $(E)^2$ for GZS:Cu crystals. (a) At the all measured range of photon energies. (b) Fitted to the best straight lines at narrow photon energies range (E^2 = 4–6 eV^2 or E = 2–2.45 eV).

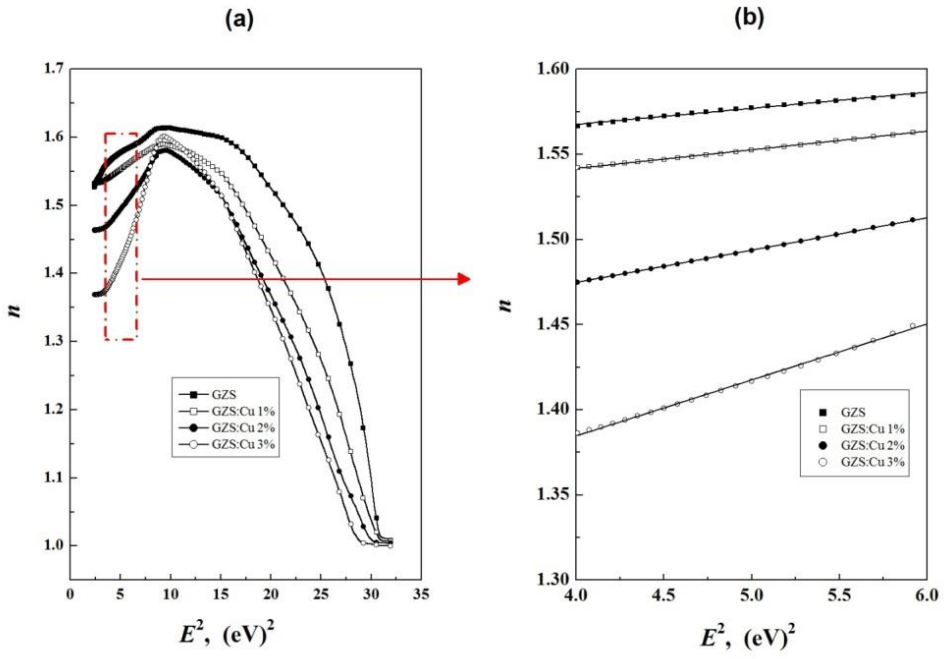

Fig. 9. Refractive index (n) versus $(E)^2$ for GZS:Cu crystals. (a) At the all measured range of photon energies. (b) Fitted to the best straight lines at narrow photon energies range (E^2 = 4–6 eV^2 or E = 2–2.45 eV).

Putting $E = 0$ in Eq. (12) gives the following equation:

$$n_0 = \left[\frac{E_d}{E_0} + 1\right]^{1/2} \quad (17)$$

Therefore, the values of E_0 and E_d in Table 2 can be used to calculate n_0 from Eq. (17) for GZS:Cu crystals. The obtained n_0 values by this method were, approximately, the same with that obtained above and listed in Table 2. This means that both Wemplee–Di-Domenico dispersion relation and Cauchy–Sellimaier dispersion equation gives the same results and, therefore, the measurements and calculations in this work have very good accuracy.

To the best of our knowledge, the normal dispersion parameters of GZS crystal are not available in the literature. Therefore, the values of normal dispersion parameters (E_0, E_d, f, M_{-1}, M_{-3}, a_1 and n_o) of pure and copper–doped GZS crystals were calculated in the present work for the first time.

Dielectric parameters

Dielectric parameters are important for materials to be used in some applications like optoelectronics. These parameters can be calculated from the optical constants obtained in previous sections. The real (ε_1) and imaginary (ε_2) parts of the complex dielectric constant (ε) are connected to the refractive index (n) and extinction coefficient ($K_{ex.}$) by the following relations [16, 19]:

$$\varepsilon = (n + iK_{ex.})^2 = \varepsilon_1 + i\varepsilon_2 \quad (18)$$

$$\varepsilon_1 = n^2 - K_{ex.}^2 \quad (19)$$

$$\varepsilon_2 = 2nK_{ex.} \quad (20)$$

Since n and $K_{ex.}$ are functions of E, ε_1 and ε_2 also depend on E. Fig. 10 (a) and (b) represent respectively such dependences for GZS:Cu crystals. For all GZS:Cu crystals and for all measured range of photon energies, the values of ε_1 are between 1 and 2.62 while the values of ε_2 are between

0 and 22 $\times 10^{-5}$. In addition, $\varepsilon_2 \cong 10^{-5}\ \varepsilon_1$ at all measured E range and for all GZS:Cu crystals. Fig. 10 (a) shows an increase of ε_1 with increasing E at the lower photon energies for all GZS:Cu crystals, and then it decreased rapidly with increasing photon energy at the higher photon energies. The part (b) of Fig. 10 shows that ε_2 decreased with increasing photon energy at the lower photon energies for all GZS:Cu crystals, and then it increased rapidly with increasing photon energy at the higher photon energies. At all measured range of photon energies, ε_1 decreased, while ε_2 increased with increasing Cu/Zn molar ratio. This behavior can be explained by increasing the conductivity of the material as a result of increasing free charge carriers in the doped crystals.

At the infrared range, ε_1 and ε_2 are related to λ^2 and λ^3 respectively as the following equations [16, 19]:

$$\varepsilon_1 \approx \varepsilon_\infty - \frac{\varepsilon_\infty \omega_p^2}{4\pi^2 c^2}\lambda^2 \quad (21)$$

$$\varepsilon_2 \approx \frac{\varepsilon_\infty \omega_p^2}{8\pi^3 c^3 \tau}\lambda^3 \quad (22)$$

where c is the velocity of light in vacuum, ε_∞ is the high frequency dielectric constant, ω_p is the plasma frequency and τ is the relaxation time. Plasma wavelength (λ_p) can be obtained from plasma frequency (ω_p) and velocity of light in vacuum (c) by using the following relation [16]:

$$\lambda_p = \frac{2\pi c}{w_p} \quad (23)$$

Fig. 11 (a) and (b) represent respectively ε_1 as a function of λ^2 and ε_2 as a function of λ^3 for GZS:Cu crystals at all measured range of wavelengths (λ = 200–800 nm). The obtained relations for ε_1 and ε_2 were fitted to the best straight lines according to Eq. (21) and Eq. (22) by using Origin program at λ range of 700–800 nm which lies at the near infrared region, as shown in insets of Fig. 11 (a) and (b) respectively. The obtained values of the high frequency dielectric constant (ε_∞), plasma frequency (ω_p), relaxation time (τ) and plasma wavelength (λ_p) for GZS:Cu crystals are listed in Table 3.

Table 3: Dielectric parameters deduced from optical measurements for GZS:Cu crystals.

	ε_∞	ω_p, (10^{14} rad.s^{-1})	τ, (10^{-12} s)	λ_p, μm
GZS	2.60	7.574	4.6348	2.487
GZS:Cu 1%	2.37	2.535	1.3953	7.431
GZS:Cu 2%	2.16	2.370	0.7007	7.948
GZS:Cu 3%	1.88	1.647	0.1521	11.44

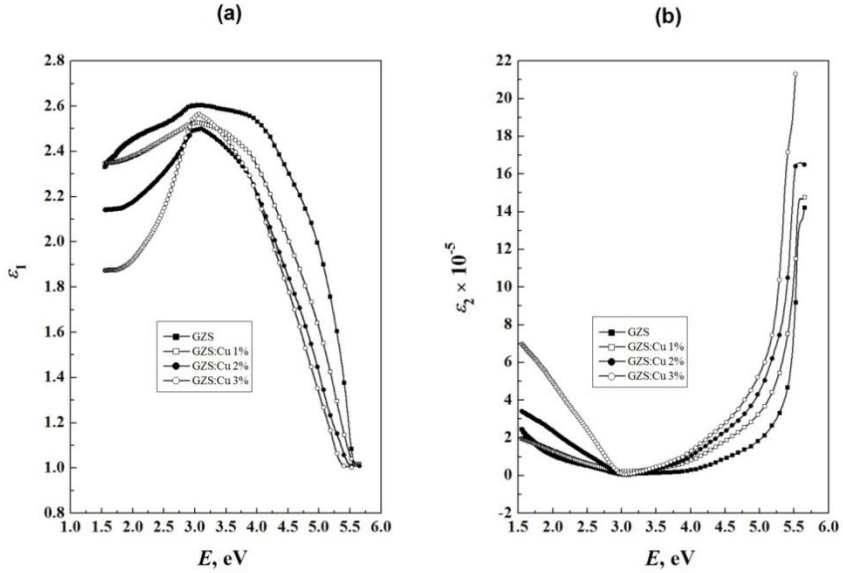

Fig. 10. Variation of the real part (a) and imaginary part (b) of complex dielectric constant with photon energy for GZS:Cu crystals.

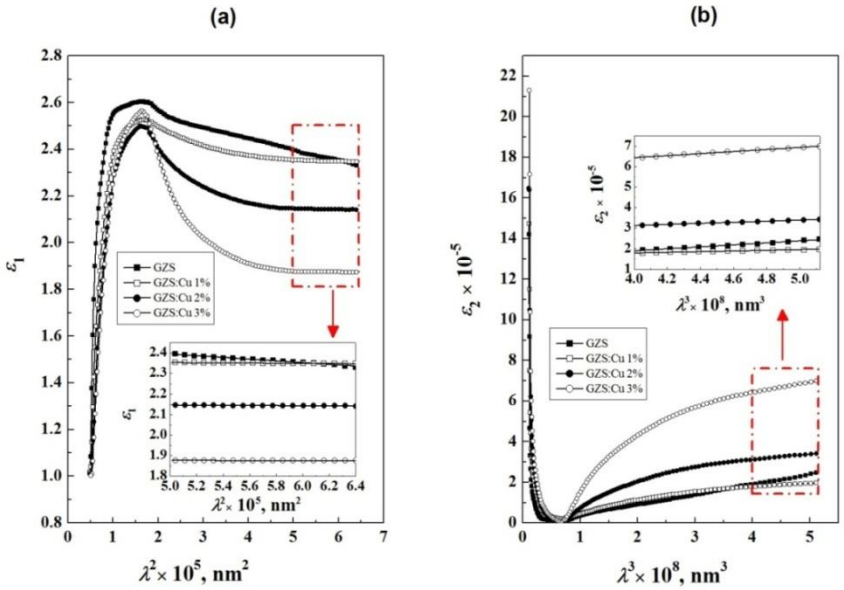

Fig. 11. Variation of the real part (a) and imaginary part (b) of complex dielectric constant with λ^2 and with λ^3 respectively for GZS:Cu crystals. The insets of (a) and (b) represent, respectively, the fitting of the obtained relations to the best straight lines at narrow wavelengths range (λ = 700–800 nm).

It is clear from Table 3 that, the high frequency dielectric constant has the highest value for the pure sample and it decreased with increasing Cu/Zn molar ratio. The same behavior is shown for plasma frequency and relaxation time while plasma wavelength has a reverse behavior. Relaxation time decreased quickly when doping GZS crystal with 1% Cu and then it decreased slowly when increasing Cu concentration to 2% and to 3%. This behavior confirmed that the electrical conduction of the crystal increased by doping it with copper.

4. Conclusions

1. One can notice from the results of this work that increasing Cu/Zn molar ratio in GZS single crystal leads to decreasing the reflection and increasing the absorption of the incident photon energy. These changes lead to decreasing E_g, n and ε_1 and increasing α, $K_{ex.}$ and ε_2. Accordingly, we can deduce that the important impact of copper dopants on the properties of GZS crystal is the decreasing of its insulating property i.e. improving its electrical conduction.
2. From the results of this work, we can notice that the changes of optical and dielectric parameters with changing Cu/Zn molar ratio are systematic (the mentioned parameters increased or decreased continuously with increasing Cu/Zn molar ratio). In addition, these changes were noticeable (have large differences) from one Cu/Zn molar ratio to another. This means that copper dopant, which had been added to the solution of growth is incorporated to GZS crystal and changes its properties i.e. the incorporation of copper ions in the lattice of GZS crystal is proportional to the Cu/Zn molar ratio in the growth solution. Therefore, Cu/Zn molar ratio in the growth solution represents the concentration of impurities or defects in the crystal lattice.
3. The dielectric parameters of GZS crystal have not been calculated yet, therefore, the values of the dielectric parameters (ε_∞, ω_p, τ and λ_p) of pure and copper–doped GZS crystals are calculated in the present work for the first time.

References

1. Abay B., Güder H. S., Yoğurtçu Y. K., (1999). Urbach–Martienssen's tails in layered semiconductor GaSe, Solid State Commun., 112: 489–494. http://dx.doi.org/10.1016/S0038-1098(99)00390-7
2. Abdulwahab A. M., (2018). Influence of cobalt-doping on the optical properties of zinc tris–thiourea sulfate (ZTS) single crystal, J. Phys. Commun., 2: 115005. https://doi.org/10.1088/2399-6528/aaecb4
3. Abdulwahab A. M., (2012). Influence of temperature on the optical properties of zinc tris-thiourea sulfate (ZTS) single crystal, Opt. Mater., 35: 146–154. http://dx.doi.org/10.1016/j.optmat.2012.07.015
4. Abu EL-Fadl A., Abdulwahab A. M., (2010). The effect of cobalt-doping on some of the optical properties of glycine zinc sulfate (GZS) single crystal, Physica B, 405: 3421–3426. http://dx.doi.org/10.1016/j.physb.2010.05.016
5. Alhuthali A., El-Nahass M. M., Atta A. A., Abd El-Raheema M. M., Elsabawy K. M., Hassanien A. M., (2015). Study of topological morphology and optical properties of SnO2 thin films deposited by RF sputtering technique, J. Lumin., 158: 165–171. http://refhub.elsevier.com/S0925-8388(16)30105-0/sref52
6. Balakrishnan T., Ramamurthi K., (2007). Structural, thermal and optical properties of a semiorganic nonlinear optical single crystal: Glycine zinc sulphate, Spectrochim. Acta, Part A, 68: 360–363. http://dx.doi.org/10.1016/j.saa.2006.12.001
7. Chitra A., Madhavan J., (2015). Growth, Structural, Thermal and Dielectric Studies of Glycine Zinc Sulphate Single Crystals, International Journal of Engineering Development and Research (IJEDR), 3: 350–353. https://www.ijedr.org/papers/IJEDR1504054.pdf
8. Elkorashy A. M., (1990). Optical Constants of Tin Sulphide Single Crystals Measured by the Interference Method, Phys. Stat. Sol. (b), 159: 903–915. http://onlinelibrary.wiley.com/doi/10.1002/pssb.2221590238/abstrac t
9. Fleck M., Bohatý L., (2004). Three novel non-centrosymmetric compounds of glycine: glycine lithium sulfate, glycine nickel dichloride dihydrate and glycine zinc sulfate trihydrate, Acta Cryst. C, 60: m291–m295. http://dx.doi.org/10.1107/S0108270104009825
10. Ganesh V., Shkir M., AlFaify S., (2019). Exploration of key physical properties of Sanakaranarayan - Ramasamy (SR) grown GZS single crystal for optoelectronic applications, Optik, 179: 207–215. https://doi.org/10.1016/j.ijleo.2018.10.158

11. Jenkins F. A., White H. E., (1957). "Fundamentals of Optics", Third Edition, McGraw-Hill Book Company, Inc., Tokyo.p49-55.
12. Keskenler E. F., Aydin S., Turgut G., Doğan S., (2014). Optical and Structural Properties of Bismuth Doped ZnO Thin Films by Sol–Gel Method: Urbach Rule as a Function of Crystal Defects, Acta Phys. Pol. A, 126: 782–786. http://dx.doi.org/10.12693/APhysPolA.126.782
13. Kumar V., Sharma S. K., Sharma T. P., Singh V., (1999). Band gap determination in thick films from reflectance measurements, Opt. Mater., 12: 115–119. https://doi.org/10.1016/S0925-3467(98)00052-4
14. Lenin M., Chandrasekar M., Udhayakumar G., (2014). Growth and characterization of nonlinear optical single crystal: Glycine zinc sulfate, Int.J. ChemTech Res., 6: 2683–2688. http://www.sphinxsai.com/framesphinxsaichemtech.htm
15. Mott N. F., Davis E. A., (1971). "Electronic Processes in Non-crystalline Materials", Oxford University Press, Oxford.
16. Mrabet C., Boukhachem A., Amlouk M., Manoubi T., (2016). Improvement of the optoelectronic properties of tin oxide transparent conductive thin films through lanthanum doping, J. Alloys Compd., 666: 392–405. http://dx.doi.org/10.1016/j.jallcom.2016.01.104
17. Nithya N., Mahalakshmi R. Sagadevan S., (2015). Investigation on Physical Properties of Semiorganic Nonlinear Optical Glycine Zinc Sulfate Single Crystal, Materials Research, 18: 581–587. http://dx.doi.org/10.1590/1516-1439.007015
18. O'Leary S. K., Zukotynski S., Perz J. M., (1997). Disorder and optical absorption in amorphous silicon and amorphous germanium, Non Cryst. Solids 210: 249–253. http://refhub.elsevier.com/S0925-8388(16)30105-0/sref48
19. Pankove J. I., (1971). "Optical Processes in Semiconductors", Prentice-Hall, New Jersey.p22-27.
20. Ravi S., Subramanian P., (2007). EPR study of Cu2+ in glycine zinc sulphate single crystal, Solid State Commun., 143: 277–279. http://dx.doi.org/10.1016/j.ssc.2007.06.003
21. Sagunthala P., Veeravazhuthi V., Yasotha P., Hemalatha P., (2016). A study on the growth of pure and zinc sulphate mono hydrate doped glycine NLO single crystals and their properties, Int. J. Chem. Sci., 14: 1041–1050. http://www.sadgurupublications.com
22. Sahadevan K., Narayansamy D., Kumaresan P., Anbarasan P. M., (2016). Effect of Swift Heavy Ion Irradiation on Coumarine Doped Glycine Zinc Sulphate (GZS) Semi Organic Crystals for Laser Applications, International Journal of Advanced Research in Physical Science (IJARPS), 3: 21–28. https://www.arcjournals.org/pdfs/ijarps/v3-i1/5.pdf
23. Sankar R., Raghavan C. M., Balaji M., Kumar R. M., Jayavel R., (2007). Synthesis and Growth of Triaquaglycinesulfatozinc (II), [Zn(SO4)(C2H5NO2)(H2O)3], a New Semiorganic Nonlinear Optical Crystal, Cryst. Growth Des., 7: 348–353. http://dx.doi.org/10.1021/cg060566k
24. Tauc J., (1974). "Amorphous and liquid semiconductors", Plenum Press, New York.p15-23.
25. Vijayalakshmi V., Dhanasekaran P., (2018). Growth and characterization study of γ-glycine crystal grown using different mole concentrations of zinc sulphate as structure-directing agents, J. Cryst. Growth 498: 372–376. https://doi.org/10.1016/j.jcrysgro.2018.07.013
26. Vijayalakshmi V., Dhanasekaran P., (2018). Optical, photoconductivity and dielectric studies of zinc sulphate added glycine crystal for photonics applications, Optik, 173: 65–70. https://doi.org/10.1016/j.ijleo.2018.08.003
27. Wemple S. H., DiDomenico M., (1971). Behavior of the Electronic Dielectric Constant in Covalent and Ionic Materials, Phys. Rev. B 3: 1338–1351. http://refhub.elsevier.com/S0925-8388(16)30105-0/sref51
28. Wooten F., (1972). "Optical Properties of Solids", Academic Press, New York.p61-68.

تأثير التطعيم بالنحاس على المعالم البصرية والعزلية لبلورات مفردة من كبريتات الخارصين جلايسين

عبده محمد عبدالوهاب[أ]*، أحمد علي صالح قايد[ب]، توفيق محمود محمد علي[ج] وأنس سعيد الشرعبي[أ]

أ) قسم الفيزياء، كلية العلوم التطبيقية، جامعة ذمار، ذمار، اليمن
ب) قسم الكيمياء، كلية العلوم التطبيقية، جامعة ذمار، ذمار، اليمن
ج) قسم الفيزياء، كلية التربية في الضالع، جامعة عدن، عدن، اليمن
* بريد إليكتروني: abduhabdulwahab@yahoo.com
DOI: https://doi.org/10.47372/uajnas.2021.n2.a09

الملخص

تم إنماء بلورات مفردة من كبريتات الخارصين جلايسين النقية والمطعمة بالنحاس بالتبخير البطيء للمحاليل المائية عند درجة حرارة ثابتة (307 كلفن)، كانت النسب المولية للنحاس إلى الخارصين هي: 1% و2% و3% في محاليل النمو، تم قياس الانعكاسية البصرية للبلورات النقية والمطعمة بالنحاس، وتم استخدامها في حساب عدة معالم بصرية وعزلية، كانت قيمة فجوة طاقة الحزمة البصرية المباشرة هي 5,44 إليكترون فولت لبلورة كبريتات الخارصين جلايسين النقية وقلت هذه القيمة مع زيادة النسب المولية للنحاس إلى الخارصين، وتم دراسة تذييل الحزمة لبلورات كبريتات الخارصين جلايسين النقية والمطعمة بالنحاس باستخدام علاقة أورباخ، وتم دراسة التفريق الطبيعي باستخدام نموذجي *Wemplee–Di-Domenico* و*Cauchy-Sellmaier*، *كما* تم أيضًا حساب الجزئيين الحقيقي والتخيلي من ثابت العزل المركب لهذه البلورات، وتم حساب معالم أورباخ ومعالم التفريق الطبيعي ومعالم العزل لبلورات كبريتات الخارصين جلايسين النقية والمطعمة بالنحاس في هذا العمل لأول مرة، تم التوصل إلى أن تطعيم بلورات كبريتات الخارصين جلايسين بالنحاس يؤثر على قيم معالمها البصرية والعزلية ويحسن توصيلها للكهرباء.

الكلمات المفتاحية: بلورات كبريتات الخارصين جلايسين، التطعيم بالنحاس، فجوة الحزمة، التفريق الطبيعي، ثابت العزل.